Spectroscopic study of the exotic nucleus ^{25}P

B. Fernández-Domínguez,[1] X. Pereira-López,[1,2] N. K. Timofeyuk,[3] P. Descouvemont,[4] W. N. Catford,[3] and F. Delaunay[2]

[1]*Universidade de Santiago de Compostela, 15754 Santiago de Compostela, Spain*

[2]*LPC Caen, ENSICAEN, Université de Caen, CNRS/IN2P3, 14050 Caen, France*

[3]*Department of Physics, Faculty of Electronics and Physical Sciences, University of Surrey, Guildford GU2 7XH, United Kingdom*

[4]*Physique Nucléaire Théorique et Physique Mathématique, C.P. 229, Université Libre de Bruxelles (ULB), B 1050 Brussels, Belgium*

(Received 31 October 2014; revised manuscript received 22 January 2015; published 9 February 2015)

Motivated by the importance of ^{25}P for the two-proton decay of ^{26}S and for searches of the mirror analog of the island of inversion near $N = 16$, we present the first predictions for the spectroscopy of the exotic isotope ^{25}P obtained in the shell model, a potential model, and a microscopic-cluster model. All models predict ^{25}P to be unbound, with an energy in the range 0.78–1.03 MeV, which favors previous mass systematics over more recent revisions. We show that ^{25}P possesses a rich low-lying spectrum that should be accessible by experimental studies. All of the predicted states below 7 MeV, except one, are narrow. Many of them are built on the excited-core states of ^{24}Si for which the Coulomb barrier is raised. For decays into the ^{24}Si(g.s.) + p channel we determined the proton widths based on their link to the asymptotic normalization coefficients (ANCs) of their mirror analogs in ^{25}Ne. We determine these ANCs from the analysis of the transfer reaction ^{24}Ne$(d,p)^{25}$Ne. The proton widths for decay into excited-state channels are obtained in model calculations. The only broad state is the intruder $3/2^-$, the mirror analog of which has been recently observed in ^{25}Ne. The ^{25}P$(3/2^-)$ energy is lower than that in ^{25}Ne, suggesting that the island of inversion may persist on the proton-rich side. All excited states of ^{25}P have at least two decay modes and are expected to populate variously the $2^+_{1,2}$ and 4^+ states in ^{24}Si, which then decay electromagnetically.

DOI: 10.1103/PhysRevC.91.024307 PACS number(s): 21.60.Gx, 23.50.+z, 27.30.+t, 21.10.Jx

I. INTRODUCTION

With the development of new radioactive beams and powerful detecting systems, the studies of exotic nuclei beyond the drip lines in light mass regions are now possible. For the neutron-rich part of the nuclear chart, the nuclei beyond the drip line generally manifest themselves as broad resonances. However, at the proton-rich side, owing to the confining nature of Coulomb barrier, the nuclear states can be narrow. Some states can be narrow because they are built on excited-core configurations. Examples of experimental evidence of such states can be found in ^{19}Na [1], ^{16}Ne [2], ^{15}F [2], ^{15}Ne [3], and ^{23}Al [4]. Theory also predicts excited-core-based narrow states in ^{17}Na [5–7] and ^{21}Al [8].

In this paper, we present a spectroscopic study of ^{25}P, a nucleus beyond the proton drip line that has the same isospin $T = 5/2$ as the two previously studied nuclei ^{17}Na and ^{21}Al. We aim to show that the ^{25}P has a rich low-lying spectrum that should be accessible to experimental study. A detailed knowledge of the ^{25}P structure would have important practical consequences. First of all, ^{25}P is a key nucleus in understanding the nature of the two-proton decay of ^{26}S, the status of which is currently unknown. Experimental searches for ^{26}S suggest that it can be a true two-proton emitter with a half-life limit of <79 ns [9]. However, the most recent phenomenological mass formula for proton-rich nuclei based on mass difference of mirror nuclei [10], predicts that one-proton emission is energetically allowed, thus favoring a sequential decay of ^{26}S via ^{25}P. A detailed knowledge of the energies and widths of the ^{25}P levels is important to understand the ^{26}S decay. Second, the mirror analog of ^{25}P, the ^{25}Ne, has signaled the need to change the widely used shell-model interaction USD, or the universal *sd*-shell interaction [11]. The need comes from the observation of the higher excitation energy of the $3/2^+_1$ and from the discovery of the intruder state $3/2^-$, which suggests an earlier onset of the evolution towards the inversion island near $N = 20$ [12]. If mirror symmetry was exact, the existence of the island of inversion and the same trend on the way to reach it would be expected on the proton-rich side of the nuclear chart. However, given that the Coulomb force gains strength with Z and T, it is not known if the island of inversion exists on the proton-rich side at all. Only recently, Togano *et al.* [13] measured a hindered proton collectivity in the $T_z = -2$ nucleus ^{28}S that indicates the emergence of a possible magic number at $Z = 16$, but no intruder states have been observed yet in this region. Besides, a measurement of the mirror energy differences for the $T = 2$ mirrors ^{36}Ca and ^{36}S [14] has shown that the evolution of the $N,Z = 16$ gap is determined by the Thomas-Ehrman shift in the $A = 17$ system with little direct influence from Coulomb effects.

Up to now, only the binding energy and S_p of ^{25}P have been calculated [9,10,15], suggesting that it is unstable with respect to proton emission. Here we present the first predictions for the ^{25}P low-lying energy spectrum. Earlier, we made the first predictions of the widths of a lighter $T = 5/2$ nucleus beyond the proton drip line, ^{21}Al [8], showing that several narrow states should be expected there. It was shown later in *ab initio* calculations [16] that the positions of the ^{21}Al levels can place important constraints on two- and three-nucleon (NN + NNN) chiral forces in nuclei. It can be expected that the ^{25}P levels will further constrain the nuclear forces.

The predictions of the ^{21}Al widths in Ref. [8] have been made by taking the theoretical positions of the proton resonances in ^{21}Al and exploiting the link between the widths of proton resonances and the asymptotic normalization coefficients (ANCs) of their mirror analogs, proposed in Ref. [17]. The ANC of the mirror analogs of ^{21}Al—the ^{21}O—have been determined from the ^{20}O$(d,p)^{21}$O reaction [18]. The ANC of the mirror analog of ^{25}P—the ^{25}Ne—can be determined in a similar fashion from a ^{24}Ne$(d,p)^{25}$Ne experiment [12]. In that publication we were interested in spectroscopic factors only. Here we determine the ^{25}Ne ANC and then use them to obtain the widths of ^{25}P for several proton energies calculated in either the shell model, the microscopic-cluster model, or a potential model. In addition, we present shell-model calculations for the γ-decay widths of the ^{25}P excited states, motivated by searches for a region in which electromagnetic decay of continuum states may become detectable. Such a region should exist because the inhibition provided by the Coulomb barrier becomes progressively more important with increasing Z.

In Sec. II we present the low-lying scheme of ^{25}Ne below 7 MeV for both experimental measurements and shell-model predictions along with three calculations of the ^{25}P spectrum using a potential model based on either shell-model energies or the measured levels of its mirror analog and a the microscopic-cluster model. In Sec. III we determine the ANC from the ^{24}Ne$(d,p)^{25}$Ne reaction. In Sec. IV we calculate the ^{25}P widths for decays into different proton channels and we compare them to the shell-model predictions for the widths of γ decay. We present our summary and conclusions in Sec. V.

II. THEORETICAL CALCULATION OF ^{25}P ENERGIES

To predict the ^{25}P spectrum we have assumed that it is related to the spectrum of its mirror analog, ^{25}Ne. For the latter, we used either the available measured energies or the predictions of the shell model. We assume that the ^{25}P levels can be obtained by adding the Coulomb interaction of a uniformly charged sphere to the standard Woods-Saxon potential well in a potential model that reproduces the ^{25}Ne energies. To explore how core excitations might affect these predictions, we have performed calculations in the microscopic-cluster model and found that their influence is not essential.

A. Experimental spectrum of ^{25}Ne

Experimental spectrum for ^{25}Ne is shown in Fig. 1. Levels with well-defined spin parity have been obtained by the TIARA collaboration [12] in the $d(^{24}\text{Ne},p\gamma)^{25}$Ne reaction using particle-γ coincidence measurements. Five bound states at ground-state (g.s.) and 1.68-, 2.03-, 3.33-, and 4.03-MeV energies have been observed. Apart from the states measured in Ref. [12], Fig. 1 includes three additional states near 3.3 MeV. A doublet with energies at 3.315 and 3.324 MeV and a state at 3.889 MeV, were observed in the β^- decay of ^{25}F [19]. Among the three levels measured in the β-decay work, only the 3.324-MeV state was tentatively assigned a spin and parity $(5/2^+)$, which was also suggested in a neutron knockout reaction from ^{26}Ne [20]. States at 4.7 and 6.2 MeV have also been observed in multinucleon transfer reactions (^{7}Li, ^{8}B) [21] and (^{13}C, ^{14}O) [22], but have not been identified.

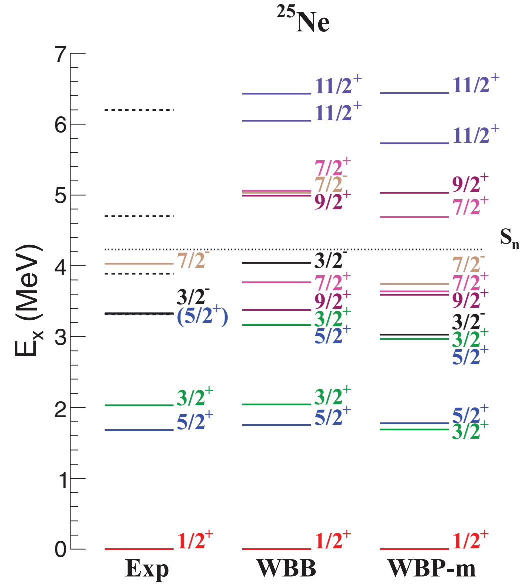

FIG. 1. (Color online) Experimental level scheme of ^{25}Ne compared to shell-model calculations using the WBB and WBP-m interactions (see text for definitions). Dashed lines correspond to states observed experimentally for which no spin and parity is available. The dotted line shows the neutron separation energy, S_n, of ^{25}Ne.

B. Shell-model spectrum of ^{25}Ne

First of all we calculate the ^{25}Ne spectrum in the shell model using the Warburton and Brown interaction [23,24]. This interaction does not include the Coulomb interaction but it should not strongly affect the ^{25}Ne, which has only two protons in the *sd* shell. The shell-model calculations were performed using the code OXBASH [25] in the full *spsdpf*-model space with two versions of the Warburton and Brown interaction: (1) the WBB that uses the universal *sd*-shell interaction B (USDB) [26] for the $2s1d$ part of the Hamiltonian and (2) the WBP-m that uses the USD [11] and the single-particle energies of the *pf* shell lowered by 0.7 MeV ito reproduce the quenching of the $N = 28$ shell gap in ^{27}Ne and the neighboring nuclei, ^{29}Mg and ^{27}Mg, as shown in Ref. [27]. In the calculations, 0 $\hbar\omega$ and 1 $\hbar\omega$ single-particle excitations of both neutrons and protons were allowed across shell gaps at $N,Z = 20$ and 8.

The results of the shell-model calculations for $J^\pi \leqslant 11/2^+$ are given in Table I and compared in Fig. 1 to the known spectrum of ^{25}Ne [12,19–22]. We also show calculated $7/2^+$, $9/2^+$, and $11/2^+$ states that are built on the 2^+ and 4^+ states of ^{24}Ne. The WBB interaction reproduces the excitation energies of ^{25}Ne$(5/2_1^+)$ and ^{25}Ne$(3/2_1^+)$ and predicts several levels around 3.3 MeV and at 4.5 MeV, where states have been observed. The predictions for ^{25}Ne made with WBP-m reproduce remarkably well the negative-parity states but for the positive-parity states the WBB is superior. Therefore, in our calculations of the ^{25}P spectrum we use the WBB interaction to estimate the proton energies for positive-parity states and the WBP-m for the negative-parity ones. We also show in Table I the shell-model spectroscopic factors that are used to

TABLE I. The shell-model energies of the ^{25}Ne levels and spectroscopic factors corresponding to the overlaps with the ground and first 2^+ and first 4^+ states in ^{24}Ne.

J_i	WBB							WBP-m						
	E_x	SF_{0^+}	$SF_{2_1^+}$					E_x	SF_{0^+}	$SF_{2_1^+}$				
			$1d_{5/2}$	$2s_{1/2}$	$1d_{3/2}$	$1f_{7/2}$	$2p_{3/2}$			$1d_{5/2}$	$2s_{1/2}$	$1d_{3/2}$	$1f_{7/2}$	$2p_{3/2}$
$1/2_1^+$	0.0	**0.64**[a]	0.84	—	0.07	—	—	0.0	0.63	0.78	—	0.08	—	—
$5/2_1^+$	1.75	**0.10**	0.03	**0.61**	0.01	—	—	1.78	0.10	0.01	0.59	0.02	—	—
$3/2_1^+$	2.04	**0.39**	0.03	**0.15**	0.02	—	—	1.69	0.48	0.06	0.07	0.08	—	—
$5/2_2^+$	3.17	**0.00**[b]	**0.07**	0.00	0.02	—	—	2.97	0.00	0.09	0.0	0.04	—	—
$3/2_2^+$	3.17	**0.22**	0.12	**0.28**	0.19	—	—	2.97	0.11	0.06	0.38	0.11	—	—
$9/2_1^+$	3.38	—	**0.05**	—	—	—	—	3.59	—	0.06	—	—	—	—
$7/2_1^+$	3.77	—	0.00	—	**0.15**	—	—	3.64	—	0.00	—	0.25	—	—
$9/2_2^+$	4.99	—	**0.03**	—	—	—	—	5.03	—	0.03	—	—	—	—
$7/2_3^+$	5.06	—	0.01	—	**0.43**	—	—	4.69	—	0.01	—	0.28	—	—
$3/2_1^-$	4.04	0.55	—	—	—	0.15	0.06	3.03	**0.53**	—	—	—	**0.16**	0.07
$7/2_1^-$	4.74	0.48	—	—	—	0.07	0.18	3.74	**0.46**	—	—	—	0.08	**0.19**
			SF_{4^+}							SF_{4^+}				
			$1d_{5/2}$	$2s_{1/2}$	$1d_{3/2}$	$1f_{7/2}$	$2p_{3/2}$			$1d_{5/2}$	$2s_{1/2}$	$1d_{3/2}$	$1f_{7/2}$	$2p_{3/2}$
$9/2_1^+$	3.38	—	0.03	**0.70**	0.02	—	—	3.59	—	0.03	0.69	0.03	—	—
$7/2_1^+$	3.77	—	0.01	**0.34**	0.06	—	—	3.64	—	0.01	0.22	0.07	—	—
$9/2_2^+$	4.99	—	0.00	**0.08**	0.00	—	—	5.03	—	0.07	0.01	0.00	—	—
$7/2_3^+$	5.06	—	0.01	**0.19**	0.03	—	—	4.69	—	0.01	0.24	0.02	—	—
$11/2_1^+$	6.05	—	0.02	—	**0.44**	—	—	4.69	—	0.03	—	0.71	—	—
$11/2_2^+$	6.43	—	0.01	—	**0.36**	—	—	5.03	—	0.02	—	0.05	—	—

[a]The SFs in bold font are those of the main components used later for computing the ^{25}P widths.
[b]The 0.00 corresponds to SF values <0.01. Only this value of 0.004 has been considered later in the calculation of the widths. The SF_{4^+} for the negative-parity states and for the $5/2_2^+$ and $3/2_2^+$ states are not shown in the table because they are <0.02 for all the orbitals. The $SF_{2_2^+}$ for the $5/2_2^+$, $3/2_2^+$, and $7/2_{1,3}^+$ states are 0.45, 0.09, 0.04, and 0.03 with a neutron in $2s_{1/2}$, $1d_{5/2}$, $1d_{3/2}$, $1d_{3/2}$, respectively. The rest of the states have $SF_{2_2^+} < 0.02$ and therefore are not used in Table II.

predict the ^{25}P widths based on a standard model that uses the single-particle widths times spectroscopic factors.

C. Potential model results for ^{25}P

Our model employs a Woods-Saxon potential of standard geometry, with the radius parameter of $r_0 = 1.25$ fm and diffuseness of $a = 0.65$ fm. The depth of this potential has been adjusted to reproduce separately the energies of each of the ^{25}Ne levels discussed in the above two sections. The results, shown in Fig. 2 and Table II, suggest that all of the states in ^{25}P are unbound with respect to proton decay. The g.s. is unbound by $\epsilon_p = 0.95$ MeV, if the potential well is chosen to fit the experimental ^{25}Ne g.s. energy, and by $\epsilon_p = 1.03$ MeV, if the potential well is chosen to fit the separation energy given by the WBB calculation. These numbers are about 200 keV smaller than those predicted by the first-order perturbation theory, which would state that the proton energy is equal to the neutron energy plus the expectation energy of the Coulomb interaction. Besides, the obtained values are much closer to the value of $Q_p = 0.840(200)$ MeV given by the previous mass compilation [28] than to the value $Q_p = 1.710(400)$ MeV from the most recent evaluation [29] or the value $Q_p = 1.507(45)$ MeV from the improved Kelson-Garvey mass relation for proton-rich nuclei [10].

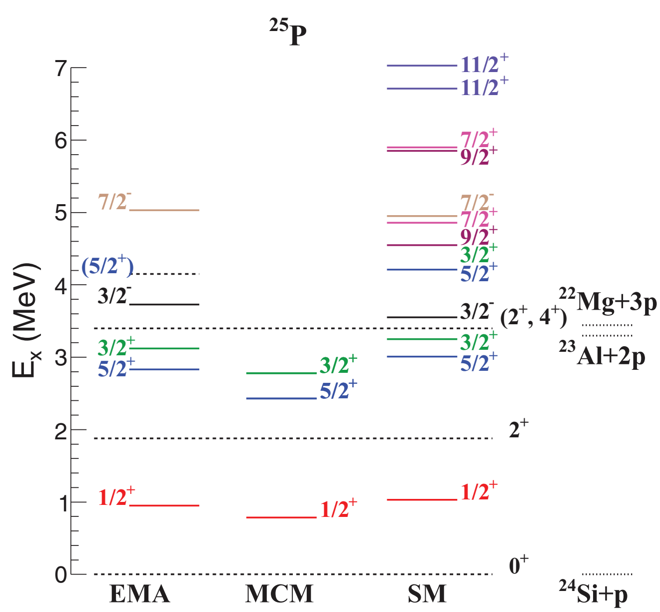

FIG. 2. (Color online) Energies ϵ_p of the resonance states in ^{25}P calculated in the potential model using either experimental energies from its mirror analog ^{25}Ne (EMA) or shell-model energies (SM) and in the microscopic-cluster model (MCM). The channels with excited cores and the one-, two-, and three-proton decay thresholds are shown by dashed lines.

TABLE II. The energies ϵ_p of the resonance states in ^{25}P calculated using the ANC from the (d,p) transfer and the shell model with either the WBB or the WBP-m interaction and with the microscopic-cluster model, MCM. The energies (in MeV) are shown with respect to the $^{24}\mathrm{Si}(0_1^+) + p$ channel. All widths are in keV.

J_i	Eq. (2)		SM					MCM		
	ϵ_p	$\Gamma_{0^+}^{(dp)}$	ϵ_p	$\mathrm{SF}_{0^+}*\Gamma_{sp}$	$\mathrm{SF}_{2_1^+}*\Gamma_{sp}$	$\mathrm{SF}_{4^+}*\Gamma_{sp}$	$\mathrm{SF}_{2_2^+}*\Gamma_{sp}$	ϵ_p	Γ_{0^+}	Γ_{2^+}
$1/2^+$	0.95	8(2)	1.03	12				0.78	2.69	
$5/2_1^+$	2.83	15(3)	3.01	13	1.8			2.43		0.16
$3/2_1^+$	3.12	52(10)	3.25	73	2.2			2.80		14.5
$5/2_2^+$			4.21	2	4		0.2			
$3/2_2^+$			4.21	118	76		0.03			
$9/2_1^+$			4.55		4	0.3				
$7/2_1^+$			4.86		10	2.4	0.10			
$9/2_2^+$			5.85		13	19				
$7/2_3^+$			5.90		191	52	1.75			
$11/2_1^+$			6.71			87				
$11/2_2^+$			7.03			100				
$3/2^-$	3.72	1059(212)	3.50	1001	0.64					
$7/2^-$	5.09	120(24)	4.96	89	51.3					

All excited states of ^{25}P are predicted to have more than one mode of decay. The $5/2_1^+$ and $3/2_1^+$ states can decay into the $^{24}\mathrm{Si}(2^+) + p$ channel as well as to the ^{24}Si(g.s.). This is true whether the experimental or the shell-model energies are used for ^{25}Ne. All the other excited states have, in addition, a third decay channel with the ^{24}Si produced in its second excited state, observed at 3.441 MeV [30]. The spin and parity of this excited state are not known but two states are known in its mirror nucleus ^{24}Ne near this energy: a 2^+ state at 3.868 MeV and a 4^+ at 3.972 MeV [31]. It would be natural to expect the existence of the mirror analogs of both of these states in ^{24}Si. Then decays of all the other predicted ^{25}P states into both the $^{24}\mathrm{Si}(2_2^+)$ and the $^{24}\mathrm{Si}(4_1^+)$ would be possible. Decay into the former state would be expected to come from the $^{25}\mathrm{P}(5/2_2^+)$ as its corresponding spectroscopic factor is 0.45 (a uniquely high value among the excited states) while decay to the latter will come from levels with spins $7/2^+$ and above. The negative-parity states, $3/2^-$ and $7/2^-$, although predicted to be above the decay thresholds for both the 2_1^+ and the 2_2^+ (or 4^+) levels in ^{24}Si will mainly decay into the g.s. channel $^{24}\mathrm{Si}(0^+) + p$ (see Table I). Finally, for all the states with the predicted proton energies above 3.4 MeV the two-proton and three-proton decay branches become possible.

D. The ^{25}P spectrum from the microscopic-cluster model

To check how core excitations may affect the prediction of the potential model, we calculate the three lowest states in ^{25}P in the microscopic-cluster model (MCM), in which the internal structures of the ^{24}Ne and ^{24}Si cores are represented by shell-model Slater determinants. We assume that nucleons in the core occupy the $d_{5/2}$ subshell only. The enormous reduction in computation time it brings makes it possible to study the effects from the excited core as both the 2^+ and 4^+ core states are possible within this scheme. The calculations are performed with the effective Volkov potential [32] traditionally used in the MCM and we adjust the strength of its Majorana part to fit the energies of each of the three lowest experimentally known ^{25}Ne states. Then with the same interaction we predict the positions of the $^{24}\mathrm{Si} + p$ resonances. This follows the spirit of the previous section but now includes the core excitations.

In the case of $1/2^+$ we adjust the Majorana strength of Volkov potential to fit the neutron separation energy in ^{25}Ne with respect to the $^{24}\mathrm{Ne} + n$ channel. However, because we used only the $d_{5/2}$ model space, both the $5/2^+$ and the $3/2^+$ are built almost purely on the $^{24}\mathrm{Ne}(2^+) + n$ configurations; therefore, for these states we adjust the Majorana interaction to fit separation energies corresponding to this channel. The location of the ^{25}P states, predicted with the MCM and shown in Fig. 2, is similar to the predictions of the potential model based on either mirror experimental or SM energies. The g.s. is slightly lower, at $\epsilon_p = 0.79$ MeV. When we exclude the core excitations from the MCM we get almost the same results as those obtained with the core excitations.

III. DETERMINATION OF ANCS FOR $^{25}\mathrm{Ne} \leftrightarrow {}^{24}\mathrm{Ne} + n$

A. Relation between neutron ANC and Γ_p

The neutron ANC is defined as the magnitude of the tail of the radial part $I_{lj}(r)$ of the overlap integral between the many-body wave functions of two neighboring nuclei $^{A}_{N}Z$ and $^{A-1}_{N-1}Z$. For a bound state of $^{A}_{N}Z$ this integral has the fundamental model-independent property that at large separations r between the nucleon and $^{A-1}_{N-1}Z$ it can be approximated as [33]

$$I_{lj}(r) \xrightarrow{r\to\infty} i^{l+1} C_n \kappa_n h_l^{(1)}(i\kappa_n r), \tag{1}$$

where $h_l^{(1)}$ is the Hankel function of the first kind [34] with orbital angular momentum l. The wave number $\kappa_n = \sqrt{2\mu\epsilon_n}/\hbar$ is determined by the neutron separation energy ϵ_n and the reduced mass μ of the last nucleon plus core. For isobar analogs of $^{A}_{N}Z$ and $^{A-1}_{N-1}Z$ the overlap $I_{lj}(r)$ has a different asymptotic behavior because at large r the Coulomb interactions between the last proton and the protons in ${}^{A-1}_{Z}(N-1)$ break down the mirror symmetry and, in particular, when ${}^{A}_{Z}N$ is unbound the asymptotics of $I_{lj}(r)$ will contain scattering waves [35–37]. At a resonance energy ϵ_p the ANC of the unbound state is directly related to the resonance width $\Gamma = |C_p|^2\kappa_p/\mu$, where $\kappa_p = \sqrt{2\mu\epsilon_p}/\hbar$. The ANCs C_p and C_n are not the same because they are associated with different asymptotic forms of $I_{lj}(r)$ in mirror channels. However, because both of them are expressed in terms of integrals over the wave functions of A and $A-1$ in the internal region [17] where the Coulomb influence is very small and, therefore, the differences in the mirror wave functions can be neglected, then a link between C_p and C_n (and, therefore, between C_n and Γ_p) can be established. It has been shown in Ref. [17] and further discussed in more detail in Refs. [36,38] that this link is given by the approximate formula

$$\frac{\Gamma_p}{C_n^2} \approx \frac{(\hbar c)^2\kappa_p}{\mu}\left|\frac{F_l(\kappa_p R_N)}{\kappa_p R_N\, j_l(i\kappa_n R_N)}\right|^2, \tag{2}$$

where F_l is the regular Coulomb wave function, j_l is the spherical Bessel function, and R_N is the range of the nuclear interaction between the last nucleon and the core $A-1$ chosen as $1.3 \times (A-1)^{1/3}$ fm. A detailed analysis of deviations of the C_p/C_n ratio from the approximate analytical formula for bound-bound mirror pairs in Ref. [36] has shown that this choice of R_N minimizes the errors of the approximation. Numerical investigations of the accuracy of Eq. (2) for the potential model and MCM performed in Refs. [36,39] suggest that Eq. (2) can overestimate the ratio Γ_p/C_n^2 on average by 10%–20%. Similar uncertainties compared to those introduced by the use of Eq. (2), i.e., in the range 10%–30% or exceptionally up to 50%, were found in other microscopic approaches [40,41] and in the coupled-channel calculations [42]. They are partially associated with the different radial extent of the mirror proton and neutron overlap integrals at large r caused by the absence or presence of the Coulomb interaction for neutron or proton, respectively. Indeed, Eq. (2) becomes much more accurate for mirror α-particle decays in which the Coulomb interaction is present in both mirror pairs making their wave functions more similar in both the internal and the external regions [38]. The possible overestimation of Eq. (2) means that the actual widths of the ^{25}P states can be smaller than the predictions of Eq. (2) and thus the ^{25}P states can live longer. Because our paper is the first study of the spectrum of the unknown isotope ^{25}P the uncertainty of the predicted widths associated with Eq. (2) is acceptable, keeping in mind that the width is in any case strongly influenced by the resonance energy. The advantage of using Eq. (2) is that it allows an estimation of the widths without any structure calculations.

B. Asymptotic normalization coefficients for ^{25}Ne

ANCs are usually determined from peripheral reactions which are sensitive only to the tails of the overlap functions $I_{lj}(r)$. Low-energy (d,p) reactions are often a good source of ANCs. We use the angular distributions of the ^{24}Ne$(d,p)^{25}$Ne reaction for five final states measured at $E =$ 10.6 MeV/nucleon [12]. The spins and parities of these states

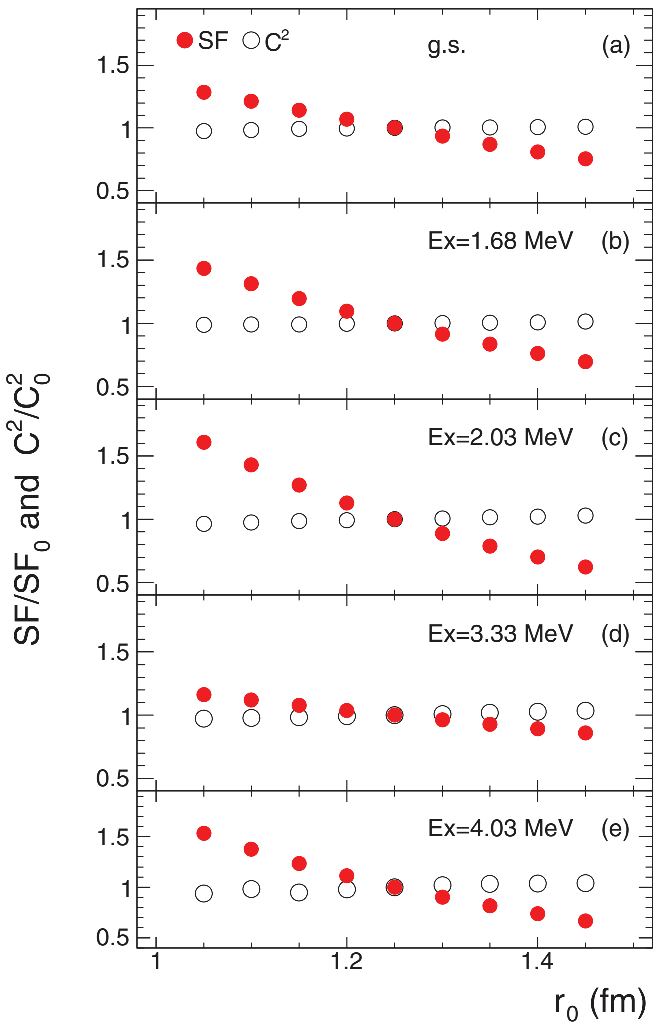

FIG. 3. (Color online) Spectroscopic factors and ANCs for the observed states of ^{25}Ne obtained for various radii of transferred neutron Woods-Saxon potential well and shown as ratios to the values obtained with the radius parameter $r_0 = 1.25$ fm.

as well as their spectroscopic factors are reported in Ref. [12]. Here we show that this reaction is peripheral and extract the ANC of the states observed. The peripherality manifests itself by independence of the results for the ANC extracted with regard to the choice of the geometry of the potential well of the bound transferred neutron. The ANC squared C_n^2 is obtained as the product of the experimental spectroscopic factors S_{lj} to the square of the single-particle ANC b_{lj} of the normalized bound-state wave function used in reaction calculations.

Theoretical calculations of the ^{24}Ne$(d,p)^{25}$Ne reaction were performed within the adiabatic distorted-wave approximation (ADWA) using the code FRESCO [43]. The adiabatic distorted potential for the $d + {}^{24}$Ne entrance channel [44] was constructed from the p-^{24}Ne and n-^{24}Ne nucleon potentials for which we used the Chapel-Hill parametrization (CH89) [45]. The same parametrization was used to generate distorted waves in the $p + {}^{25}$Ne channel. The neutron single-particle form factors were obtained using a Woods-Saxon potential with the depth adjusted to reproduce the experimental separation

TABLE III. Asymptotic normalization coefficients squared C_n^2 (in fm^{-1}) obtained from the ^{24}Ne $(0^+)(d,p)^{25}$Ne (J_f^π) reaction.

J_f^π	lj	$C^2_{(d,p)}$
$1/2_1^+$	$s_{1/2}$	12.0 ± 0.2
$5/2_1^+$	$d_{5/2}$	0.04 ± 0.01
$3/2_1^+$	$d_{3/2}$	0.07 ± 0.01
$3/2_1^-$	$p_{3/2}$	0.35 ± 0.07
$7/2_1^-$	$f_{7/2}$	$5.7 \pm 1.1 \times 10^{-6}$

energies of the observed levels. The radius parameter of this potential was varied to investigate the peripheral character of the reaction. Figure 3 shows the weak dependence of the extracted ANC on the binding potential geometry. The variation in the ANC over the full range presented here is less than 3%. The ANCs obtained within the ADWA for five states are presented in the Table III. The relative errors shown in this table are the same as in previous work [12].

IV. CALCULATION OF ^{25}P WIDTHS

A. Proton partial widths

The ^{25}Ne ANC obtained above and the relation (2) have been used to predict the proton widths of ^{25}P assuming that the proton resonance energies come from the potential model adjusted according to the experimental spectrum of ^{25}Ne observed in the (d,p) reaction. These proton widths are listed in Table II, suggesting that four mirror analogs of the ^{25}Ne states—namely, the $1/2^+$, $5/2^+$, $3/2^+$, and $7/2^-$ states—are narrow and should be observed to have widths that are much smaller than the spacing between adjacent states. The mirror analog of the ^{25}Ne$(3/2^-)$ intruder is broad but nevertheless should be identifiable experimentally, albeit with some possible overlap with the lower $3/2^+$ energy level.

In a more sophisticated model, the MCM (in which core excitations are included), the ^{25}P g.s. energy is smaller and, therefore, this state is even narrower but its width corresponds to a lifetime that is still well below the upper limit of the experimental half-life of 30 ns given in Ref. [28] and confirmed subsequently at Dubna [9]. The MCM predicts also small widths for decay of excited states $5/2^+$ and $3/2^+$ into the ^{24}Si$(2_1^+) + p$ channel.

We also calculate the widths of the ^{25}P states predicted by the potential model when based upon the shell-model calculations for ^{25}Ne. These levels are shown in Fig. 2. The widths were obtained as $\Gamma_p = \mathrm{SF} \times \Gamma_{\mathrm{s.p.}}$, where $\Gamma_{\mathrm{s.p.}}$ denotes the single-particle width obtained from the scattering phase-shift at the resonance energy in a Woods-Saxon potential tuned to reproduce the calculated separation energy of a chosen ^{25}Ne level, and SFs are the spectroscopic factors from Table I. Spectroscopic factors for mirror pairs are assumed to be equal, according to the charge symmetry of the strong interaction. In Table II we show the shell-model widths for decay into four channels: 0^+, $2^+_{1,2}$, and 4^+. To get the energy of the decay to the 2_1^+ we used the known ^{24}Si(2_1^+) value. Because we do not know where the 2_2^+ and the 4^+ states are located, we assumed that both of them lie at 3.44 MeV, where a level was observed with unknown spin and parity. We see that the proton-decay widths of the resonances are small relative to the spacing between levels, at low excitation energy. At high excitation energies, the level density predicted by the shell model is expected to be high and the widths might well cause the overlap of several energy levels.

TABLE IV. Γ_γ partial widths of the electromagnetic decays. λ is the multipolarity of the transition.

$O\lambda : I_i \rightarrow I_f$	WBB Γ_γ(keV)	WBP-m Γ_γ(keV)
$E2 : 5/2^+ \rightarrow 1/2^+$	5.47×10^{-7}	6.25×10^{-7}
$M1 : 3/2^+ \rightarrow 1/2^+$	2.42×10^{-6}	2.01×10^{-6}
$E1 : 3/2^- \rightarrow 1/2^+$	3.72×10^{-4}	1.13×10^{-4}
$E1 : 7/2^- \rightarrow 5/2^+$	3.23×10^{-7}	2.17×10^{-7}

B. Γ partial widths

We have checked if the γ-ray emission from the ^{25}P excited states is sufficiently strong to be detectable. For this purpose we have performed shell-model calculations for reduced transition probabilities $B(O_\lambda; I_i \rightarrow I_f)$ and the corresponding γ widths Γ_γ for a few ^{25}P levels, assuming isospin symmetry. We expect that such calculations will give correct predictions for the order of magnitude of Γ_γ. The largest widths are shown in Table IV both for the WBB and WBP-m interactions. We can see that the largest width can be associated with the $E1$ transitions from the intruder state ^{25}P$(3/2^-)$. The $M1$ transition from ^{25}P$(3/2^+)$ is two orders of magnitude weaker. All electromagnetic widths are much smaller than the proton-decay widths by at least five orders of magnitude. This shows that the Coulomb barrier at $Z = 15$ is not strong enough to open competition between the proton decay and γ emission. Because at a typical experiment we can expect about a few hundred events corresponding to the population of excited states of ^{25}P there is no chance to observe a weak electromagnetic branch. Therefore, all γ rays detected in reactions populating ^{25}P should come from the deexcitation of the ^{24}Si core.

V. SUMMARY AND CONCLUSIONS

We have presented the first detailed study of the spectrum of the unbound isotope ^{25}P using its link to the known spectrum of its mirror analog ^{25}Ne and performing several model calculations. All models suggest that ^{25}P should be unbound with respect to the proton decay ^{24}Si + p by 0.78–1.0 MeV, which is compatible with the estimate of $Q_p > 0.23$ MeV obtained from the experimental search for proton emission from ^{25}P in Ref. [9]. However, our estimates favor the values of $Q_p = 0.840(200)$ MeV from older mass systematics from Ref. [28] rather than the latest higher values of $Q_p = 1.710(400)$ MeV and $Q_p = 1.507(45)$ MeV from the latest works of Refs. [29] and [10], respectively. Smaller values of Q_p could affect the theoretical predictions of the two-proton energy in ^{26}S.

Our calculations have demonstrated that ^{25}P has a rich low-lying spectrum composed by states narrow enough to be observed experimentally. In the region $E_p < 7$ MeV all the predicted states, except for the intruder state $3/2^-$, have their widths much smaller than the resonance energies. These widths normally do not exceed 100 keV, which is either smaller or comparable to a typical resolution in modern experiments with radioactive beams. Only the g.s. of ^{25}P is expected to have a single decay mode, namely, ^{24}Si(g.s.) + p. The $5/2_1^+$ and $3/2_1^+$, being mainly based on an excited-core configuration, will have the additional decay mode of ^{24}Si$(2^+) + p$. All the other states should also have important decay modes to either 2_2^+ or 4^+ excited states in ^{24}Si. One candidate state is known in ^{24}Si around 3.4 MeV seen in the ^{28}Si$(\alpha,{}^8$He$)^{24}$Si reaction [30] and it lies above the particle emission threshold. Experimental observation of γ rays in Ref. [46] suggests that it lives long enough with respect to the particle decay to make the competition with γ emission possible. Populating the ^{24}Si states through the particle decay from ^{25}P combined with the information about the ^{25}P in future experiments as well as measuring various branching ratios will give a unique opportunity to study the spectroscopy of both ^{25}P and ^{24}Si in the same experiment and, in particular, to observe the excited-core content of ^{25}P. Then, using mirror relations, the ANC of excited ^{25}Ne states to excited ^{24}Ne states, where particle decays are not energetically allowed, can be determined indirectly. This will shed light into the structure of ^{25}Ne, for which any experiments aimed to measure these quantities are not possible as they would require radioactive beams of short-lived excited states.

The only broad state predicted in the low-lying spectrum of ^{25}P should be the intruder $3/2^-$. It should lie just below 4 MeV and have a width of about 1 MeV. Our calculations predict a lowering of this state owing to the Thomas-Ehrman shift with respect to its observed mirror analog in ^{25}Ne. Measuring the position of the $3/2^-$ intruder in ^{25}P will help to answer the question about whether the mirror analog of the neutron-rich island of inversion near $N = 16$ exists. It has already been experimentally demonstrated that mirror symmetry in the disappearance of the magic number 8 persists between the $T = 2$ nucleus ^{12}O and its mirror ^{12}Be [47]. It would be natural to expect the persistence of the island of inversion. The position of $3/2^-$ is also relevant to the intruder content in ^{26}S. Currently, the p^2 content of ^{26}S is predicted by the relativistic mean field approach (RMF) to be less than 10% for realistic values of the pairing gap [9] although the energies of the intruders are not cited there. A possible increase of the weight of intruders can affect the lifetime of ^{26}S with respect to the proton emission.

Finally, we would like to comment on possible experiments in which the ^{25}P can be studied. This is, first of all, the proton scattering in inverse kinematics, ^{24}Si + p.

This experiment is expected to populate the mirror analogs of the states seen in transfer reaction ^{24}Ne$(d,p)^{25}$Ne. These are the first three positive-parity narrow states and a narrow negative-parity $7/2^-$ state. These should be well separated and observed as individual resonances. They should be observed in interference with a wide intruder $3/2^-$ state. By measuring the excitation energies at different angles, coupled with the standard R-matrix analysis, it should be possible to disentangle the energies and the widths of these resonances. The states with higher spin parities can, in principle, be seen in a three-proton transfer reaction with a radioactive ^{22}Mg beam, although the small cross sections for this reaction will make such an experiment unlikely in the near future. Also, because the predicted level density of these states is higher, some of them would be not resolved.

ACKNOWLEDGMENTS

We wish to thank Prof. B. A. Brown for assisting us with the shell-model calculations. B.F.D. acknowledges financial support from the Ramón y Cajal program of the Spanish Ministerio de Ciencia e Innovación under Contract No. RYC-2010-06484. N.K.T. and W.N.C. are grateful for UK STFC Grant No. ST/J000051/1. One of the authors, X.P.L., wishes to acknowledge the support of an IN2P3/CNRS doctoral fellowship.

[1] M. G. Pellegriti *et al.*, Phys. Lett. B **659**, 864 (2008).
[2] I. Mukha *et al.*, Phys. Rev. C **79**, 061301(R) (2009); **82**, 054315 (2010).
[3] F. Warmers *et al.*, Phys. Rev. Lett. **112**, 132502 (2014).
[4] A. Gade *et al.*, Phys. Lett. B **666**, 218 (2008).
[5] N. K. Timofeyuk and P. Descouvemont, Phys. Rev. C **81**, 051301(R) (2010).
[6] H. T. Fortune and R. Sherr, Phys. Rev. C **82**, 027310 (2010).
[7] K. Amos *et al.*, Nucl. Phys. A **879**, 132 (2012).
[8] N. K. Timofeyuk, B. Fernandez-Dominguez, P. Descouvemont, W. N. Catford, F. Delaunay, and J. S. Thomas, Phys. Rev. C **86**, 034305(R) (2012).
[9] A. S. Fomichev *et al.*, Int. J. Mod. Phys. E **20**, 1491 (2011).
[10] J. Tian, N. Wang, Ch. Li, and J. Li, Phys. Rev. C **87**, 014313 (2013).
[11] B. A. Brown and B. H. Wildenthal, Annu. Rev. Nucl. Part. Sci. **38**, 29 (1988).
[12] W. N. Catford *et al.*, Phys. Rev. Lett. **104**, 192501 (2010).
[13] Y. Togano *et al.*, Phys. Rev. Lett. **108**, 222501 (2012).
[14] P. Doonenbal *et al.*, Phys. Lett. B **647**, 237 (2007).
[15] B. A. Brown and P. G. Hansen, Phys. Lett. B **381**, 391 (1996).
[16] J. D. Holt, J. Menendez, and A. Schwenk, Phys. Rev. Lett. **110**, 022502 (2013).
[17] N. K. Timofeyuk, R. C. Johnson, and A. M. Mukhamedzhanov, Phys. Rev. Lett. **91**, 232501 (2003).
[18] B. Fernández-Domínguez *et al.*, Phys. Rev. C **84**, 011301(R) (2011).
[19] S. W. Padgett *et al.*, Phys. Rev. C **72**, 064330 (2005).
[20] J. R. Terry *et al.*, Phys. Lett. B **640**, 86 (2006).
[21] K. H. Wilcox *et al.*, Phys. Rev. Lett. **30**, 866 (1973).
[22] C. L. Woods, L. K. Fifield, R. A. Bark, P. V. Drumm, and M. A. C. Hotchkis, Nucl. Phys. A **437**, 454 (1985).
[23] E. K. Warburton and B. A. Brown, Phys. Rev. C **46**, 923 (1992).
[24] E. K. Warburton, J. A. Becker, and B. A. Brown, Phys. Rev. C **41**, 1147 (1990).
[25] http://www.nscl.msu.edu/ brown/resources/resources.html.

[26] B. A. Brown and W. A. Richter, Phys. Rev. C **74**, 034315 (2006).
[27] S. M. Brown *et al.*, Phys. Rev. C **85**, 011302(R) (2012).
[28] G. Audi, A. H. Wapstra, and C. Thibault, Nucl. Phys. A **729**, 337 (2003).
[29] M. Wang *et al.*, Chin. Phys. C **36**, 1603 (2012).
[30] H. Schatz *et al.*, Phys. Rev. Lett. **79**, 3845 (1997).
[31] A. J. Howard *et al.*, Phys. Rev. C **1**, 1446 (1970).
[32] A. B. Volkov, Nucl. Phys. **74**, 33 (1965).
[33] J. M. Bang, F. G. Gareev, W. T. Rinkston, and J. S. Vaagen, Phys. Rep. **125**, 253 (1985).
[34] M. Abramowitz and I. A. Stegun (eds.), *Handbook of Mathematical Functions with Formulas, Graphs, and Mathematical Tables* (Dover Publications, New York, 1972).
[35] A. M. Mukhamedzhanov and R. E. Tribble, Phys. Rev. C **59**, 3418 (1999).
[36] N. K. Timofeyuk and P. Descouvemont, Phys. Rev. C **72**, 064324 (2005).
[37] K. M. Nollett, Phys. Rev. C **86**, 044330 (2012).
[38] N. K. Timofeyuk, P. Descouvemont, and R. C. Johnson, Phys. Rev. C **75**, 034302 (2007).
[39] N. K. Timofeyuk, P. Descouvemont and R. C. Johnson, Eur. Phys. J. **27**, 269 (2006).
[40] J. Okolowicz, N. Michel, W. Nazarewicz, and M. Ploszajczak, Phys. Rev. C **85**, 064320 (2012).
[41] K. M. Nollett and R. B. Wiringa, Phys. Rev. C **83**, 041001(R) (2011).
[42] L. J. Titus, P. Capel, and F. M. Nunes, Phys. Rev. C **84**, 035805 (2011).
[43] I. J. Thompson, Comput. Phys. Rep. **7**, 167 (1988).
[44] R. C. Johnson and P. C. Tandy, Nucl. Phys. A **235**, 56 (1974).
[45] R. L. Varner *et al.*, Phys. Rep. **201**, 57 (1991).
[46] K. Yoneda *et al.*, Phys. Rev. C **74**, 021303(R) (2006).
[47] D. Suzuki *et al.*, Phys. Rev. Lett. **103**, 152503 (2009).